Toward Ubiquitous Connectivity via LoRaWAN: An Overview of Signal Collision Resolving Solutions

Chenglong Shao, Osamu Muta, Wenjie Wang, and Wonjun Lee

Abstract

The ever increasing demand for energy-efficient, long-range, and license-free Internet of Things (IoT) communication networks has spurred great interest in unlicensed low-power wide area networks (LPWANs). Such a revolutionary technology represents a paradigm shift in the development of wireless networks, as it can enable low-power (milliwatts) IoT devices to transmit at low data rates (kilobits per second) over long distances (several kilometers), which is clearly different from conventional IoT networking technologies (e.g., Wi-Fi and ZigBee) that only support short-range communications. Specifically, long-range WAN (LoRaWAN) is a leading and representative LPWAN technology that has been gathering remarkable attention from both academia and industry because of its open source software and installation ease. Despite this interest, however, current LoRaWAN is not yet a mature communication platform to provide ubiquitous connectivity for a wide variety of IoT applications. This is mainly because LoRaWAN typically serves a large volume of coexisting end devices among which signal collisions frequently occur at the physical layer (LoRa) of LoRaWAN, thereby leading to severe degradation of overall network capacity. In this context, the aim of this article is to provide a comprehensive overview of up-to-date physical-layer solutions for LoRa collision resolution. We particularly investigate different types of LoRa collisions resulting from the spreading factor network parameter. Moreover, the potential visions of physical-layer design to resolve LoRa collisions that might be considered for future research are also discussed.

Introduction

The past few years have witnessed the prosperity of low-power wide area networks (LPWANs) as a promising networking paradigm to provide Internet connectivity for various Internet of Things (IoT) devices. Their emergence stems from their combination of low-power and long-range features that are key requirements of IoT applications. Specifically, by operating in the unlicensed frequency bands (e.g., 868 MHz and 915 MHz), unlicensed LPWANs further facilitate their installation to allow arbitrary users to deploy their own networks and enable various do-it-yourself projects.

Among several unlicensed LPWAN technologies, long-range WAN (LoRaWAN) is perhaps the most representative. It basically serves a large volume of coexisting end devices for physical-world sensing, several gateways mainly for sensed data collection, and back-end network/application servers for data analysis. LoRaWAN has been deployed in more than 170 countries for various industrial applications such as power usage monitoring and waste management. It is also attractive to academic research because of its deployment ease and open source software.

Despite this interest, deploying large-scale LoRaWAN is still a challenging task. This is mainly because current LoRaWAN simply adopts pure ALOHA protocol for wireless channel access. This protocol allows end devices to occupy LoRaWAN channels for their own transmissions upon having data to send [1]. Since a LoRaWAN gateway usually serves a large volume of end devices, this will inevitably lead to frequent collisions among the transmissions of coexisting end devices, which statistically limits achievable network capacity up to only 18 percent of the maximum, even in the optimal case [1].

Bearing this in mind, researchers have made several efforts from the perspective of the LoRaWAN data link layer for signal collision avoidance. For example, instead of the pure ALOHA protocol used in current LoRaWAN, a time-division multiple access (TDMA)-based channel access control protocol is described in [2]. To achieve random channel access among coexisting LoRaWAN end devices, carrier sense multiple access (CSMA) based on a newly introduced LoRaWAN function called channel activity detection is proposed in [3]. Aside from their improvements, these approaches entail software modifications on both end devices and gateways. They also increase computational overhead and energy cost, particularly on the resource-constrained end devices.

To avoid the drawbacks above, physical-layer (PHY) design of LoRaWAN has been flourishing over the past four years. This type of technique focuses on resolving the collisions when they have already arisen. Specifically, software modifications are needed only on LoRaWAN gateways, which maintains the deployment and upgrade ease of LoRaWAN. In this context, the goal of this article is to review this branch of research on emerging LoRaWAN PHY design for signal collision resolution in a comprehensive manner. We start with a brief summary of the key features in LoRaWAN PHY that are useful to understand the reasons behind LoRa collisions. In particular, due to the diverse settings on a LoRaWAN parameter called spreading factor (SF), we consider two signal collision types together for the first time: collisions under different SFs and collisions under identical SF. Thus, we then conduct practical experiments to explain how these two types of collisions happen and present corresponding collision resolution techniques, respectively. Finally, by considering the limitations and margin of improvement of the reviewed PHY solutions, we discuss some future research directions that we deem worthy of further investigation. We then draw the conclusion.

LoRaWAN PHY: LoRa

LoRaWAN defines the communication protocol and system architecture for the network while its PHY, called LoRa, enables its long-range communication link. This section summarizes the key features of LoRa typically exploited for LoRa collision resolution.

Chenglong Shao and Osamu Muta are with Kyushu University, Japan.
Wenjie Wang is with Xi'an Jiaotong University, China.
Wonjun Lee is with Korea University, Republic of Korea.

Digital Object Identifier: 10.1109/IOTM.001.2100114

 2576-3180/21/$25.00 © 2021 IEEE

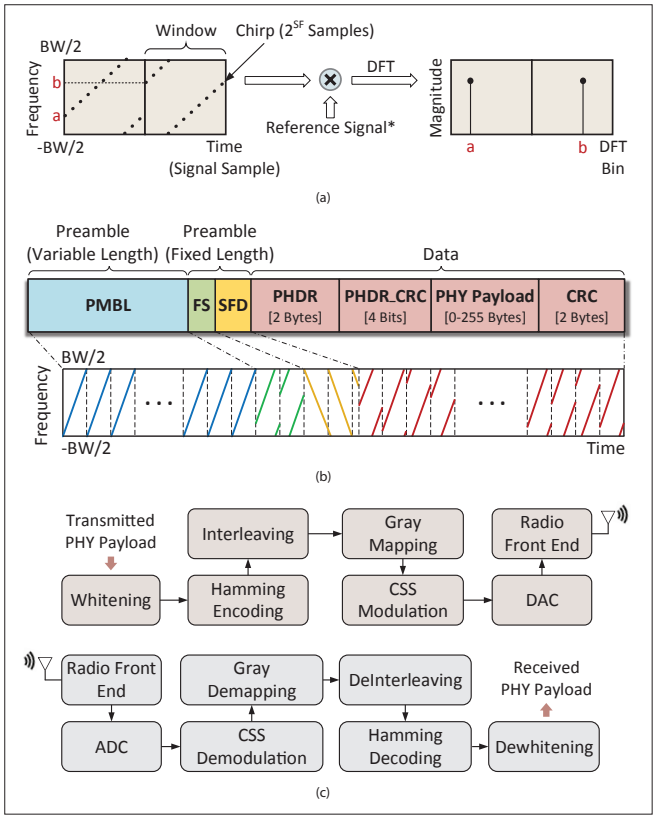

FIGURE 1. LoRa signal transmission and reception: a) CSS modulation and demodulation; each peak bin after demodulation indicates the initial frequency of the corresponding chirp; b) LoRa packet format; the CRC field is only present in uplink transmissions; c) generic block diagrams of LoRa transmitter and receiver. DAC: digital-to-analog converter; ADC: analog-to-digital converter.

LoRa Modulation and Demodulation

LoRa signals are modulated with the scheme called chirp spread spectrum (CSS). As depicted in Fig. 1a, a CSS-modulated signal is split into successive time windows, and the signal within a window is called a chirp. Basically, the frequency of a chirp increases linearly with time within the bandwidth (BW). After the frequency reaches BW/2, it returns to −BW/2 and continues to increase. The number of signal samples within a chirp is typically set to be 2^{SF}. In LoRa, SF (typically 7–12) represents spreading factor and indicates the number of data bits contained in a chirp. The initial frequency of a chirp corresponds to the transmitted data.

For signal demodulation, LoRa can multiply each received chirp with the complex conjugate of a reference signal. Typically, this reference signal is an unmodulated upchirp whose frequency spreads from −BW/2 to BW/2. This will transform the received chirp into a sinusoid of constant frequency. LoRa then applies down-sampling and discrete Fourier transform (DFT) to this sinusoid. This results in a clear DFT peak bin whose index indicates the contained data.

LoRa Packet Format

As shown in Fig. 1b, a LoRa packet starts with PMBL, a preamble with variable length used for signal arrival detection. In the following preamble with fixed length, two fields exist: Frame Sync (FS) for packet synchronization and Start Frame Delimiter (SFD) for frequency offset compensation. Specifically, FS and SFD are required to consist of 2 modulated upchirps and 2.25 unmodulated downchirps, respectively, whose frequency simply spreads from BW/2 to −BW/2.

After SFD, the packet contains its carried data composed of multiple modulated upchirps. The PHY Header (PHDR) indicates the meta information of the data such as data length and coding rate (CR). It is associated with PHDR_CRC, a cyclic redundancy check (CRC) field for PHDR bit error detection. The following PHY payload indicates the data received from upper layers of LoRaWAN. In the case of uplink transmissions from LoRaWAN end devices to gateways, LoRa additionally derives a 16-bit CRC based on the PHY payload.

LoRa Transceiver

As provided in Fig. 1c, the LoRa transmitting chain includes data whitening, Hamming encoding, interleaving, and reverse Gray mapping. Their operations in the receiving chain are in the reverse direction. Data whitening aims to remove direct current (DC)-bias in the transmitted data via a predefined pseudo-random sequence. Given PHDR, PHDR_CRC, whitened PHY payload, and CRC, Hamming encoding is applied so that bit errors observed in the receiving chain can be corrected automatically. The available Hamming CR is 4/5, 4/6, 4/7, or 4/8. Only 4/8 is allowed in PHDR and PHDR_CRC so that they can be decoded correctly with a high chance. The following interleaving operation focuses on avoiding successive bit errors in the receiving chain by distributing the bits of a LoRa chirp among multiple chirps. Gray mapping is used to make the data correspond to two adjacent DFT bins with only a single-bit difference.

LoRa Collision Resolution under Different SFs

One of the key features of LoRa is that two LoRa signals based on different SFs do not interfere with each other in principle. Figure 2a gives an example where our targeted SF10-based chirp experiences interference from two SF9-based chirps. These two traces of chirps were generated with our GNU Radio software-based CSS modulator that adheres to its standard implementation in LoRa. They were combined together and then transmitted via a USRP N210 software-defined radio (SDR). Note that the two traces feature the same signal strength; that is, signal-to-interference ratio (SIR) is set to 0 dB. We built a CSS demodulator with GNU Radio and USRP N210 SDR. The experiment was conducted in an indoor scenario corresponding to a typical office environment (5.5 m × 5 m). The LoRa transmission proceeded in LoRa uplink channel 63 with center frequency of 914.9 MHz and BW of 125 kHz. The demodulation result in Fig. 2b illustrates that there is a clear peak DFT bin corresponding to the carried data of our target chirp regardless of the interference. However, this property does not always hold in practical LoRaWAN, and the following presents an example of how the problem of LoRa collisions occurs when different SFs are adopted.

Problem Briefing

In LoRaWAN, SF allocation is basically performed based on the distances between end devices and a gateway. The end devices with longer distances to a gateway typically adopt higher SFs. In this context, when a nearby end device and a remote one transmit simultaneously with different SFs, it is highly possible that the configuration of SIR = 0 dB cannot be satisfied. Thus, with the same hardware, software, and parameter settings as used for Fig. 2a, we further conduct an experiment regarding the chirp collision between SF10 and SF9 with the setting of SIR = −25 dB, as shown in Fig. 2c. The result in Fig. 2d shows that the SF9-based interfering chirps add considerable noise to the result, and simply searching the peak bin for our targeted data retrieval might lead to demodulation error.

Enabling Techniques

While an example of LoRa collisions under different SFs is provided above, it is typically assumed that LoRa signals under different SFs are orthogonal to each other. Thus, developing the corresponding collision resolution techniques is still an open topic to be widely studied with no specific approach proposed yet. It is

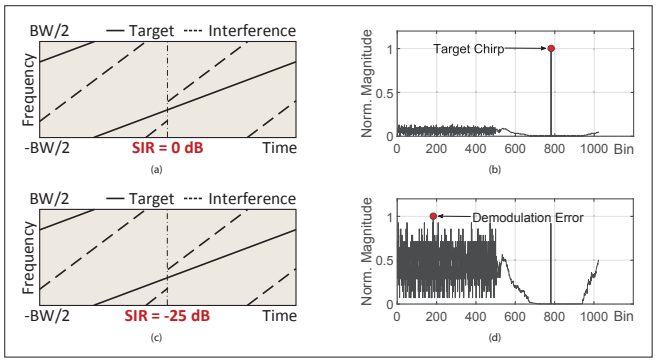

FIGURE 2. LoRa signal collisions under different SFs (Target: SF10; Interference: SF9): a) chirp collision with SIR = 0 dB; b) normalized DFT result under SIR = 0 dB; c) chirp collision with SIR = −25 dB; d) normalized DFT result under SIR = −25 dB.

	SF_{int}					
	7	8	9	10	11	12
$SF_{tgt} = 7$	X	−8	−9	−9	−9	−9
$SF_{tgt} = 8$	−11	X	−11	−12	−13	−13
$SF_{tgt} = 9$	−15	−13	X	−13	−14	−15
$SF_{tgt} = 10$	−19	−18	−17	X	−17	−18
$SF_{tgt} = 11$	−22	−22	−21	−20	X	−20
$SF^{tgt} = 12$	−25	−25	−25	−24	−23	X

TABLE 1. SIR threshold (dB) regarding LoRa signal collisions under different combinations of SFs [4].

worth noting that a relative study regarding the measurement of imperfect orthogonality between different SFs is presented in [4]. In particular, given LoRa collisions under different combinations of SFs, experiment-based SIR thresholds below which the interfering SF-based signals incur severe demodulation error are provided in Table 1. It can be seen that given a certain interfering SF (SF_{int}), the SIR threshold decreases as larger target SFs (SF_{tgt}) are adopted. This accords with the fact that LoRa signals with larger SFs are more robust to signal degradation caused by wireless channel fading, interference, and so forth. Note that the SIR thresholds in Table 1 are reference or empirical values rather than exact or theoretical ones. They can be affected by various factors such as the carried data bits of LoRa signals, experiment environment, and used LoRa hardware. Based on this result and our experimental observations in Fig. 2, we believe that one promising PHY design direction to resolve this type of collisions is to distinguish the DFT bin indicating our target signal from the ones caused by the interference before searching the peak bin for target data decoding. More details are provided later.

LoRa Collision Resolution under Identical SF

LoRa signals modulated with the same SF basically interfere with each other when they fully or partially overlap during reception. The following provides an example of how this problem happens.

Problem Briefing

To figure out the underlying reasons behind LoRa collisions under identical SF, we conduct an experiment with the same hardware, software, parameters, and wireless environment described earlier. Given a certain overlapping pattern of two SF10-based signal traces, Figs. 3a and 3c show the chirp collisions with the settings of SIR = −1 dB and SIR = −3 dB, respectively. The corresponding demodulation results in Figs. 3b and 3d illustrate that reduced SIR may also lead to demodulation error when the same SF is adopted. We also figure out that the interference corresponds to clear DFT bins, and the bin height is highly related to the signal overlapping pattern. In this context, we fix SIR to be 0 dB and change the overlapping pattern as shown in Figs. 3e and 3g. The overlapping pattern is determined via the change of packet offset (PO), that is, the sample offset between the two signal traces with the demodulation window as a benchmark. Figures 3f and 3h show that the height of a DFT bin is approximately proportional to the length of the corresponding chirp within the demodulation window. As a result, we can conclude that even the setting of SIR = 0 dB can typically lead to signal collision if the colliding signals are perfectly aligned.

Enabling Techniques

By considering the LoRa collision reasons above, academia's quest to solve this type of LoRa collisions has emerged recently. Specifically, we choose several representative solutions [5–14] as up-to-date and noteworthy approaches tailor-made for collision resolution of LoRa signals. Generally, they aim to distinguish the target DFT bin from the interfering bins and then conduct standard LoRa decoding operations to extract target information. We provide a brief summary of them as follows, and then analyze their performance and limitations in a comparative manner.

- Choir [5]: As the first-ever research effort to combat LoRa collisions under identical SF, Choir exploits hardware imperfections of LoRaWAN devices. To be more specific, two LoRa signals transmitted from two devices basically experience different frequency offsets at a receiver. This is because the oscillators in the transmitters and the receiver can hardly operate with the same oscillating frequency. Consequently, in comparison with the DFT bins resulting from a standard size (2^{SF}) of DFT operation, small bin position shifts can be seen when a larger size (10×2^{SF}) of DFT is performed. More importantly, a certain transmitter corresponds to a fixed position shift throughout its associated chirps/bins, and this shift is typically unique for each transmitter. Based on this observation, Choir achieves correct mapping between the DFT bins and the transmitters, thereby successfully disentangling LoRa collisions.
- SS5G [6]: By assuming that collided LoRa signals are slightly desynchronized, SS5G aims to detect sharp frequency edge in the time domain in addition to the standard recognition of DFT bins in the frequency domain. Recalling the LoRa modulation scheme depicted in Fig. 1a, the sharp frequency edge stems from sudden frequency change that may arise at the beginning of a chirp or within the chirp. According to the sharp frequency edges, SS5G introduces several time points to split collided signals into multiple segments and performs DFT to obtain segment-wise DFT bins. These bins are then compared and updated through the analysis of successive segments to determine the final data bits carried by the collided signals.
- mLoRa [7]: Unlike the frequency-domain recognition of collided LoRa signals above, mLoRa takes the first effort to separate LoRa collisions in the time domain. The key motivation of the design of mLoRa is that due to the use of CSS modulation in LoRa, chirp waveform adheres to a known pattern that can be regarded as a reference to recover contaminated signal samples in the time domain. Specifically, since signal collision usually has a time offset between the overlapped signals, several collision-free signal samples may exist at the beginning of the collision. Based on these samples and the known chirp waveform, mLoRa can estimate the following collided samples associated with the corresponding chirp. By subtracting the estimated samples from the collision, mLoRa can then obtain collision-free samples belonging to another signal.
- FTrack [8]: Figure 3 shows that the resulting DFT bin of a chirp corresponds to the initial frequency of the chirp even when the demodulation window is misaligned with the chirp. Based on this observation, FTrack introduces the concept of frequency track representing the instantaneous frequency components within a certain demodulation window. This information is obtained by employing a moving demodulation window in a sample-by-sam-

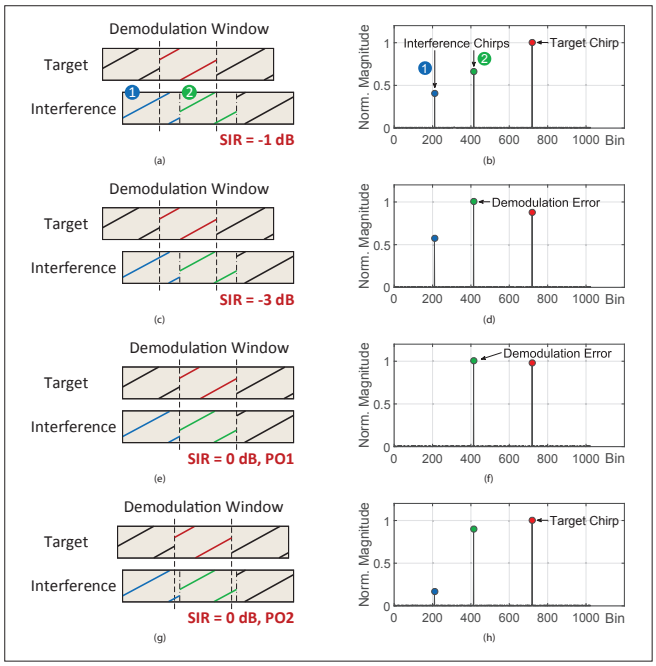

FIGURE 3. LoRa collisions under identical SF (SF10): a) chirp collision with a certain overlapping pattern and SIR = −1 dB; b) normalized DFT result regarding a); c) chirp collision with the same overlapping pattern as a) and SIR = −3 dB; d) normalized DFT result regarding c); e) chirp collision with SIR = 0 dB and PO1; f) normalized DFT result regarding e); g) chirp collision with SIR = 0 dB and PO2; h) normalized DFT result regarding g).

ple manner and performing standard DFT within each window. FTrack can measure the length of each segment in the frequency track to recognize signal collision, signal preamble, and data portion. In particular, since a signal collision has a certain overlapping pattern, segments in the frequency track appear to be superimposed in a similar manner. Thus, FTrack groups the segments into multiple sets corresponding to different transmitters and then conducts individual decoding.

- CoLoRa [9]: Based on the fact that the overlapping pattern in a LoRa collision does not change, CoLoRa aims to derive the ratio of the segment lengths regarding a single chirp caused by the misalignment between the chirp and the demodulation window. With no need for chirp synchronization, CoLoRa simply employs successive demodulation windows to split collided signals. In the case that the demodulation window is not perfectly aligned with a chirp, the resulting DFT bins in two contiguous demodulation windows will have the same frequency. In this context, CoLoRa can know that the two DFT bins correspond to the same chirp and then calculate the ratio between the two bins. Since it is proved that the bin height is proportional to the chirp segment length, this ratio is used to group DFT bins for each signal, and the standard LoRa decoding is performed accordingly.
- NScale [10]: Instead of the standard reference signal used for LoRa demodulation, NScale explores the feasibility of adopting a different reference signal for LoRa collision resolution. Specifically, the reference signal is designed to be the standard one with varying amplitude along time, which leads to scaled DFT bins after the corresponding DFT operation. By combining the results with the DFT bins obtained via the standard reference signal, NScale can then derive the scaling factor associated with each bin. Since the scaling factor is proved to be related to the chirp length within the demodulation window, it can be regarded as an indicator of the overlapping pattern of a signal collision. Due to the unchanged overlapping pattern throughout a collision, the DFT bins can be groups for each signal according to their associated scaling factors, and individual LoRa decoding can be performed thereafter.
- FlipLoRa [11]: Recalling the CSS demodulation process, it is known that applying DFT to the multiplication result between an arbitrary upchirp (downchirp) and an unmodulated upchirp (downchirp) does not yield a peak bin. In other words, when a chirp is multiplied with the same type (up or down) of unmodulated chirp, its energy will be spread over the whole spectrum rather than being accumulated in a certain frequency. Based on this fact, FlipLoRa encodes a LoRa packet as interleaved upchirps and downchirps instead of upchirps only. In this way, when a two-signal-based LoRa collision occurs and the demodulation window is perfectly aligned with the chirps of one of the two signals, it can be seen that the DFT results in two contiguous demodulation windows containing a single peak bin and two peak bins, respectively. By comparing the corresponding frequencies of the three bins, FlipLoRa can then recognize and decode the collided chirps.
- SCLoRa [12]: Given that it is hard to discriminate collided chirps of a single DFT operation within a demodulation window, SCLoRa resorts to calculating cumulative spectral coefficient, which ix distribution of power information associated with a certain DFT bin. This is done by sliding the demodulation window back and forth and performing DFT within each demodulation window. Based on the obtained cumulative spectral coefficient and the frequency offset information derived from the corresponding PMBL field, SCLoRa can pinpoint the bin of each chirp and accordingly extract the carried data bits. For signal separation, SCLoRa evaluates the bin power information of the unmodulated upchirps in the PMBL field. This feature is typically distinct for different signals since they generally have different signal strength. Furthermore, SCLoRa takes into consideration the spectrum leakage problem caused by the insufficiency of sliding windows and opts for rectangular window and Blackman window as the window functions to address this problem.
- Pyramid [13]: After performing preamble-based LoRa packet detection, Pyramid leverages a sliding window within which collided LoRa chirps are transformed into multiple peak bins in the frequency domain based on the DFT-based CSS demodulation operation. Since the peak height of a single chirp is proportional to the intersection degree between the chirp and the window, the trajectory of the peak height along the position of the window turns out to be an isosceles triangle theoretically. Specifically, the apex of the triangle corresponds to the case when the window is perfectly aligned with the chirp. The localization of an apex is achieved via linear regression due to the existence of noise. Moreover, the interval between two apexes associated with two consecutive chirps of the same packet is equal to the chirp length. In this context, Pyramid can classify colliding chirps into different packets based on the inter-apex interval and extract the data contained in the packets that have collided.
- CIC [14]: Given a target LoRa signal overlapping with multiple interfering ones, CIC first determines the chirp boundary of each signal by detecting their preambles. CIC then leverages multiple CSS demodulation window pieces smaller than the standard one with the same duration as a chirp. In particular, the positions of these window pieces are set based on the obtained chirp boundaries of the involved signals. In this context, CIC selects the collided sub-chirps within several window pieces so that the interfering sub-chirps are different across all of them. Consequently, after the DFT-based CSS demodulation of each sub-chirp, only the DFT bin of the target signal chirp is common across the demodulation results of all the selected sub-chirps. Thus, an intersection operation among the spectral information of the selected sub-chirps can remove all the interfering DFT bins and leave behind only the target bin for final decoding.

Solution	Year	Type	Key technique	Computational cost	Evaluation approach	Two-signal collision		Tolerable number of collisions
						CER (%)	Throughput (chirps/s)	
Choir [5]	2017	Decoding only	Frequency offset recognition	High	SDR + LoRa chip	N/A	50 (SF7)	10 (PLR: 42%)
SS5G [6]	2019	Decoding only	Sharp frequency edge detection	Low	Simulation	N/A	19.2 (SF12)	8 (PLR: 13%)
mLoRa [7]	2019	Decoding only	Sample-wise estimation	Medium	SDR	5 (SF8)	22.5 (SF8)	3 (CER: 9%)
FTrack [8]	2020	Decoding only	"Frequency track" generation	High	SDR + LoRa chip	7–9 (SF8)	50 (SF8)	10 (CER: 14%)
CoLoRa [9]	2020	Decoding only	Contiguous DFT bin ratio analysis	Low	SDR + LoRa chip	N/A	14.2 (SF12)	20 (PLR: 30%)
NScale [10]	2020	Decoding only	Non-stationary DFT bin scaling	Medium	SDR + LoRa chip	7–28 (SF8)	49–61 (SF10)	10 (CER: 6%)
FlipLoRa [11]	2020	Encoding and decoding	Up-down chirp interleaving	High	Simulation & SDR	0 (SF12)	17.5 (SF12)	5 (CER: 6%)
SCLoRa [12]	2020	Decoding only	"Cumulative spectral coefficient" evaluation	High	SDR + LoRa chip	5 (SF8)	50 (SF8)	10 (CER: 46%)
Pyramid [13]	2021	Decoding only	Peak tracking and apex localization	High	SDR + LoRa chip	1 (SF12)	47 (SF12)	7 (CER: 41%)
CIC [14]	2021	Decoding only	"Spectral intersection" computation	Medium	SDR + LoRa chip	6 (SF8)	N/A	N/A

TABLE 2. Solution comparison regarding LoRa collisions under identical SF.

Regarding the existing solutions above, we further make a comprehensive comparison shown in Table 2. The high computational cost of Choir, FTrack, FlipLoRa, SCLoRa, and Pyramid results from very large DFT (Choir), sample-wise moving CSS demodulation (FTrack), modifications at both end devices and gateways (FlipLoRa), and sliding-window-based repeated DFT (SCLoRa and Pyramid). With these resource-consuming and complicated operations sidestepped, the computational cost is reduced for the other techniques, among which SS5G and CoLoRa are the relatively lightweight ones. In comparison to mLoRa, NScale, and CIC, which entail pre-processing of each collided signal sample before demodulation (mLoRa) and multi-time CSS demodulation for each chirp (NScale and CIC) respectively, SS5G and CoLoRa achieve collision resolution with one-time CSS demodulation for each chirp in a demodulate-as-sample-comes manner. Furthermore, since these techniques are evaluated with different SFs and performance metrics adopted, we specifically provide the underlying SF in Table 2 regarding the chirp error rate (CER) and throughput. Specifically, CER refers to the ratio between erroneous chirps and totally transmitted chirps in a certain interval when all the observed collisions are caused by two signals. The throughput refers to the number of successfully decoded chirps in a second on average when only two LoRa end devices transmit concurrently. Note that the values of CER and the throughput are extracted directly from the corresponding studies. We also associate the tolerable number of collisions (the maximum number of signals in a collision that can be successfully decoded as described in [5–13]) with the corresponding performance to achieve more comprehensive description of the capability of each solution. Note that Choir, SS5G, and CoLoRa opt for packet loss rate (PLR) as the performance metric.

Future Research Directions

After presenting an overview of the existing solutions for LoRa collision resolution, we provide several PHY opportunities to inspire further research on this topic. As described below, two are for the collisions under different SFs and one is for the case of identical SF.

Successive Interference Cancellation

Recalling that LoRa collisions between different SFs are mainly caused by signal strength unbalance as explained earlier, the conventional technique of successive interference cancellation (SIC) can be a possible solution. Note that while current SIC-based solutions (e.g., [15]) for LoRa collision resolution target collisions under identical SF, this technique could also be employed for collisions under different SFs. Generally, the SIC approach performs as follows:

1. Decoding the strongest signal in the collision
2. Recovering the strongest signal and subtracting it from the collision
3. Repeating the former two steps until no collision

In LoRa collisions under different SFs, SF_{tgt} is typically much less than SF_{int}. Thus, the interference can be regarded as the strongest signal to decode first, as depicted in Fig. 4a. In particular, given a LoRa receiver configured with SF_{tgt} to receive the signals under the same SF, this approach requires the receiver to try all possible SFs during signal arrival detection to recognize SF_{int}.

Adaptive DFT Bin Denoising

Despite the feasibility of the SIC-based solution above, the "interference first" type of collision resolution inevitably leads to tremendous additional computational overhead. Accordingly, it is more desirable to directly extract the target signal irrespective of the data contained in the interference. Given the collision shown in Figs. 2c and 2d, DFT bin denoising can be achieved as depicted in Fig. 4b, since our target chirp corresponds to a DFT bin that is clearly separated from the noisy ones caused by the interference. However, this operation is highly likely to fail if our target bin turns out to be mixed with the noisy ones. This can be caused by the carried data of the LoRa chirps or severe channel fading that strongly distorts the magnitudes and phases of signal samples. One plausible solution is to perform cross-chirp bin power comparison as illustrated in Fig. 4b. This is based on the fact that among all the demodulation results from a certain collision, it is highly possible that there is one where our target bin and noisy bins are clearly separated, as shown in Fig. 2d. Thus, since our target bins have similar power, we can use the magnitude of the target bin as a threshold to filter out the bins with lower magnitudes in the demodulation result where our target is hard to recognize.

Two-Dimensional Chirp Mapping

Regarding LoRa signal collisions under identical SF, we look forward to devising a more lightweight solution than the existing ones by reducing the arithmetic of multiplication and divi-

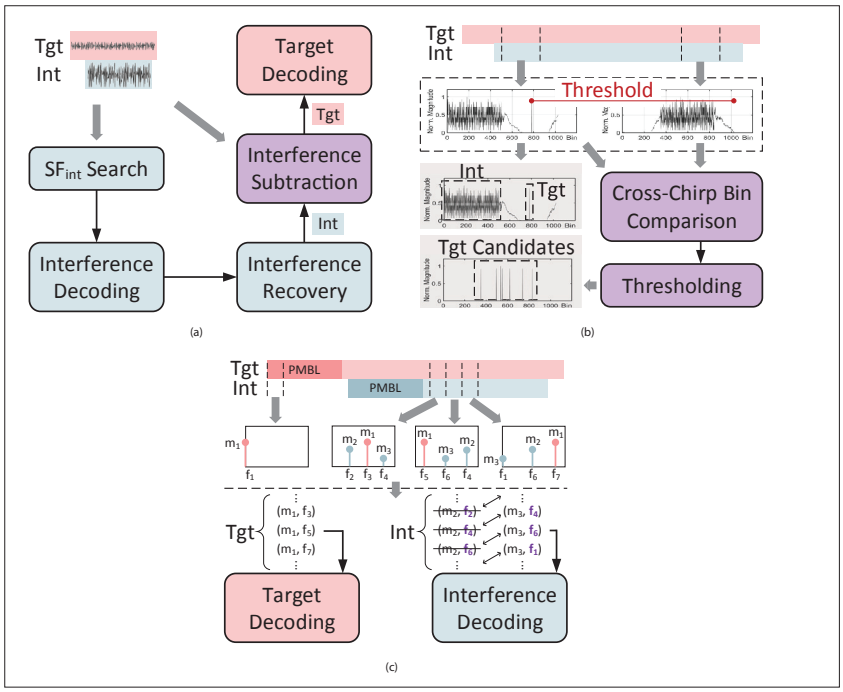

FIGURE 4. Research opportunities against different types of LoRa collisions: a) SIC for collision resolution under different SFs; b) adaptive DFT bin denoising for collision resolution under different SFs; c) two-dimensional chirp mapping for collision resolution under identical SF. Tgt: target; Int: interference.

sion among signal samples and DFT bins. Recall that when the demodulation window is perfectly aligned with the chirps of a LoRa signal, the resulting DFT bins will have approximately the same magnitude. Thus, if the PMBL field of the signal is free of collision, the magnitude of its DFT bins can be regarded as a reference to map subsequent bins to the same signal. When the demodulation window is misaligned with LoRa chirps, a chirp corresponds to two DFT bins; thus, it is hard to simply use the PMBL field for chirp mapping. In this case, one possible solution is to generate two separate groups of bins, as depicted in Fig. 4c. Given two bin groups, it is only necessary to observe the frequencies of bins from two contiguous demodulated windows in different groups. Since a chirp corresponds to a certain bin frequency with different bin magnitudes, one of the two bin groups can simply be neglected, and another one is used to decode the interfering signal. In this magnitude-frequency-based way, collided chirps can be mapped to their associated signals without the need for multiplication and division.

Conclusion

This article takes the PHY perspective to explore the fact that current LoRaWAN is still unable to serve as a mature network architecture for ubiquitous IoT connectivity. We first investigate the key PHY reasons behind the drawbacks of LoRaWAN, which are manifested in LoRa signal collisions. We then review the corresponding collision resolution techniques in the literature. Finally, we provide several research insights for different types of LoRa collisions. Since PHY design for LoRa collision resolution typically requires no modification at LoRaWAN end devices, we believe that this approach will provide a very cost-effective path to ubiquitous IoT connectivity and hybrid global IoT coverage.

Acknowledgment

This work was supported in part by the Japan Society for the Promotion of Science (JSPS) Postdoctoral Fellowships for Research in Japan (No. 21F21074).

References

[1] N. Abramson, "The ALOHA System: Another Alternative for Computer Communications," *Proc. ACM*, Nov. 17–19, 1970, Fall Joint Comp. Conf., 1970.
[2] K. Q. Abdelfadeel *et al.*, "FREE — Fine-Grained Scheduling for Reliable and Energy-Efficient Data Collection in LoRaWAN," *IEEE IoT J.*, vol. 7, no. 1, Jan. 2020, pp. 669–83.
[3] A. Gamage *et al.*, "LMAC: Efficient Carrier-Sense Multiple Access for LoRa," *Proc. ACM MobiCom*, 2020.
[4] D. Croce *et al.*, "Impact of LoRa Imperfect Orthogonality: Analysis of Link-Level Performance," *IEEE Commun. Lett.*, vol. 22, no. 4, Apr. 2018, pp. 796–99.
[5] R. Eletreby *et al.*, "Empowering Low-Power Wide Area Networks in Urban Settings," *Proc. ACM SIGCOMM*, 2017.
[6] N. El Rachkidy, A. Guitton, and M. Kaneko, "Collision Resolution Protocol for Delay and Energy Efficient LoRa Networks," *IEEE Trans. Green Commun. Net.*, vol. 3, no. 2, June 2019, pp. 535–51.
[7] X. Wang *et al.*, "mLoRa: A Multi-Packet Reception Protocol in LoRa Networks," *Proc. IEEE ICNP*, 2019.
[8] X. Xia, Y. Zheng, and T. Gu, "FTrack: Parallel Decoding for LoRa Transmissions," *IEEE/ACM Trans. Net.*, vol. 28, no. 6, Dec. 2020, pp. 2573–86.
[9] S. Tong, Z. Xu, and J. Wang, "CoLoRa: Enabling Multi-Packet Reception in LoRa," *Proc. IEEE INFOCOM*, 2020.
[10] S. Tong, J. Wang, and Y. Liu, "Combating Packet Collisions Using Nonstationary Signal Scaling in LoRa Networks," *Proc. ACM MobiSys*, 2020.
[11] Z. Xu *et al.*, "FlipLoRa: Resolving Collisions with Up-Down Quasi-Orthogonality," *Proc. IEEE SECON*, 2020.
[12] B. Hu *et al.*, "SCLoRa: Leveraging Multi-Dimensionality in Decoding Collided LoRa Transmissions," *Proc. IEEE ICNP*, 2020.
[13] Z. Xu, P. Xie, and J. Wang, "Pyramid: Real-Time LoRa Collision Decoding with Peak Tracking," *Proc. IEEE INFOCOM*, 2021.
[14] M. O. Shahid *et al.*, "Concurrent Interference Cancellation: Decoding Multi-Packet Collisions in LoRa," *Proc. ACM SIGCOMM*, 2021.
[15] D. Garlisi *et al.*, "Interference Cancellation for LoRa Gateways and Impact on Network Capacity," *IEEE Access*, vol. 9, 2021, pp. 128,133–46.

Biographies

Chenglong Shao [M'18] (shao@mobcom.ait.kyushu-u.ac.jp) received his B.S. degree in information and communications engineering from Xi'an Jiaotong University, Shaanxi, China, in 2010. He received his Ph.D. degree in computer science and engineering from Korea University, Seoul, Republic of Korea, in 2019. After serving as a research professor in the Future Network Center of Korea University, he joined Kyushu University, Fukuoka, Japan, in 2021, where he is currently a JSPS international research fellow in the Center for Japan-Egypt Cooperation in Science and Technology. His research interests include wireless networking, mobile computing, and wireless security.

Osamu Muta (muta@ait.kyushu-u.ac.jp) received his associate B.E. degree from Sasebo Institute of Technology in 1994, his B.E. degree from Ehime University in 1996, his M.E. degree from Kyushu Institute of Technology in 1998, and his Ph.D. degree from Kyushu University in 2001. In 2001, he joined the Graduate School of Information Science and Electrical Engineering, Kyushu University as an assistant professor. Since 2010, he has been an associate professor in the Center for Japan-Egypt Cooperation in Science and Technology, Kyushu University. His current research interests include signal processing for wireless communications and power line communications, MIMO, interference coordination, and nonlinear distortion compensation for high-power amplifiers.

Wenjie Wang (wjwang@xjtu.edu.cn) received his B.S., M.S., and Ph.D. degrees in information and communication engineering from Xi'an Jiaotong University in 1993, 1998, and 2001, respectively. He was a visiting scholar with the Department of Electrical and Computer Engineering, University of Delaware, Newark, from 2009 to 2010. He is currently a professor at Xi'an Jiaotong University. His main research interests include information theory, broadband wireless communications, signal processing with application to communication systems, array signal processing, and cooperative communications in distributed networks.

Wonjun Lee [M'00, SM'06, F'21] (wlee@korea.ac.kr) received his B.S. and M.S. degrees in computer engineering from Seoul National University, Republic of Korea, in 1989 and 1991, respectively; his M.S. degree in computer science from the University of Maryland, College Park in 1996; and his Ph.D. degree in computer science and engineering from the University of Minnesota, Minneapolis in 1999. In 2002, he joined the Faculty of Korea University, where he is currently a professor with the School of Cybersecurity. His research interests include network protocols, optimization in wireless networking, security in mobile computing, and RF-powered computing.